

MATERIALS AND INTERFACES

Chemistry and Structure of the Passive Film on Mild Steel in CO₂ Corrosion EnvironmentsJiabin Han,[†] David Young,^{*†} Hendrik Colijn,[‡] Akhilesh Tripathi,[§] and Srdjan Nešić[†]

Institute for Corrosion and Multiphase Technology (ICMT), Department of Chemical and Biomolecular Engineering, Ohio University, Athens, Ohio 45701, The OSU Campus Electron Optics Facility, The Ohio State University, Columbus, Ohio 43210, and Rigaku Americas Corp., 9009 New Trails Drive, The Woodlands, Texas 77381

The passivation process was carried out and monitored employing a three electrode electrochemical glass cell. Surface analysis using grazing incidence X-ray diffraction (GIXRD) elucidated that trace magnetite in the dominant siderite (FeCO₃) was responsible for the passivation. Transmission electron microscopy (TEM) with the energy dispersive X-ray fluorescence (EDX) technique was used to determine the structure of the passive layer and confirm its chemistry. A passive phase tens of nanometers thick was observed beneath iron carbonate scale and at the crystal boundaries. Scanning transmission electron microscopy (STEM)/EDX profiles suggest that this phase is not a carbonate containing compound since only oxygen and iron were observed. This indicates that the possible chemical compound for the passive phase is an iron oxide, agreeing with the previous GIXRD surface analysis. Fe₃O₄ as a passive film was confirmed.

1. Introduction

Grazing incidence X-ray diffraction (GIXRD) is an important characterization method for identification of thin films on a surface. The penetration depth in an asymmetric (2θ) GIXRD analysis is well-controlled and is based on incident angle compared to conventional symmetric (θ/θ) X-ray diffraction.^{1–3} GIXRD enhances diffraction from the outer thin layer of the analyzed surface and minimizes diffraction from the substrate.

Transmission electron microscopy (TEM) or scanning transmission electron microscopy (STEM) can image surfaces at subnanometer resolution.⁴ Combined with EDX analysis, elemental chemistry information can be obtained.

In principle, the methodology outlined herein could be applied to study the reactivity of any metal surface. The study outlined in this paper shows how GIXRD combined with electrochemical measurements can be used to explain reactivity and corrosion of a mild steel surface in a typical corrosion environment. TEM together with EDX can be used to determine the fine structure and chemistry of complex layered scales. The chosen system involved passive film formation on mild steel in CO₂ saturated electrolyte, a typical sweet corrosion environment.

Classically, passivation can generally be distinguished from immunity by electrochemical definitions. For noble metals such as platinum and gold, the bare metal maintains corrosion resistivity up to relatively high potentials. This differs from what is observed for active metals such as aluminum and titanium, corrosion resistivity is obtained at a higher potential due to formation of a thin passivating compact film. In ongoing research by the current authors, spontaneous passivation has been observed for mild steel in CO₂ aqueous media.⁵ The conditions correspond to an actively corroding metal under

typical CO₂ aqueous environments, as acknowledged by the open literature.⁶ The process of passivation occurred “naturally”, when compared with passivation artificially achieved by external application of potential or current,^{7,8} as described in the definition of passivation *vide supra*.

The analysis of the passive film formed on mild steel in CO₂ environments was necessary to understand the mechanisms of uniform and localized CO₂ corrosion. This film formed under particular conditions can protect steel from severe corrosion. The passive film can also lead to localized corrosion as a result of its partial breakdown.^{5,9} Ferrous oxide [FeO], ferrous hydroxide [Fe(OH)₂], magnetite [Fe₃O₄], or ferric hydroxide [Fe(OH)₃] have been proposed to be responsible for the passivation of the metal in H₂O–iron environments, under both aerobic and anaerobic conditions.⁷ FeCO₃, also known as siderite, was proposed as a phase which had “the potential to form passive films” in the H₂O–CO₂–Fe system by Heuer.⁸ Carbonate containing compounds including Fe₂(OH)₂CO₃ and Fe₂O₂CO₃ were proposed to be passive-layer forming by De Marco and co-workers.¹⁰ Guo and Tomae observed trace Fe₃O₄/Fe(OH)₂ in the dominant FeCO₃ scale.¹¹

In the current study, phase composition and the structure of the spontaneous passive film formed on mild steel exposed to CO₂ saturated solutions were expected to be identified with the aid of GIXRD and TEM/EDX, in order to help advance the understanding of phenomena that underpin passivation in this corrosion environment.

2. Experimental Procedures

The spontaneous passivation tests were conducted in a three electrode electrochemical glass cell⁶ as depicted in Figure 1.

The key components of the cell are labeled as follows: (1) condenser, (2) reference electrode, (3) pH probe, (4) Luggin capillary, (5) platinum ring counter electrode, (6) working electrode, (7) thermo probe, (8) gas bubbler, (9) magnetic stirrer bar, (10) hot plate. Mild/carbon steel coupons were used to

* To whom correspondence should be addressed. E-mail: dyoung@bobcat.ent.ohiou.edu. Tel.: +1 740 593 9944. Fax: +1 740 593 9945.

[†] Ohio University.

[‡] The Ohio State University.

[§] Rigaku Americas Corp.

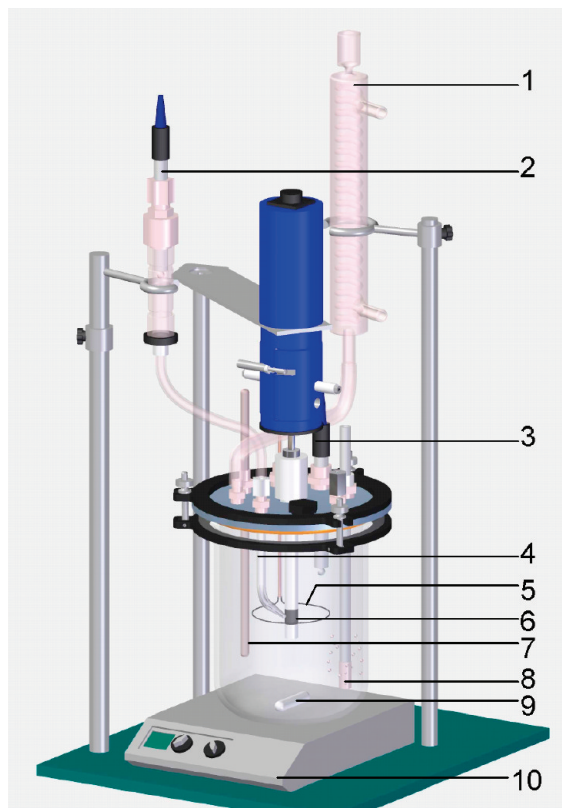


Figure 1. Three electrode electrochemical glass cell.⁶ Reproduced with permission from the ICMT image library.

Table 1. Chemical Composition (weight percent) for X65 Mild Steel

Al	As	B	C
0.00322	0.005	0.0003	0.05
Ca	Co	Cr	Cu
0.004	0.006	0.042	0.019
Mn	Mo	Nb	Ni
1.32	0.031	0.046	0.039
P	Pb	S	Sb
0.013	0.02	0.002	0.011
Si	Sn	Ta	Ti
0.31	0.001	0.007	0.002
V	Zr	Fe	
0.055	0.003	balance	

produce the working electrode. The potential was measured with reference to the saturated Ag/AgCl reference electrode. The counter electrode was made out of a platinum ring. This setup is a universal apparatus for electrochemical study of metal reactivity, at ambient pressure and temperatures that do not exceed solution boiling points.

Sodium chloride electrolyte (1 wt %) was prepared, heated to 80 °C, and deaerated with sparging by carbon dioxide. The pH of the solution was adjusted to pH 8.0 by addition of solid NaHCO₃ (ACROS, ACS analytical grade 99.7%) in order to speed up the formation of FeCO₃ scale and passive film. Mild steel, X65 (composition shown in Table 1), corrosion coupons were polished sequentially by 200, 400, and 600 grit silicon carbide abrasive paper. This sample was used for GIXRD/XRD analysis. The sample used for TEM/EDX analysis was

Table 2. Chemical Composition (weight percent) for C1018 Carbon Steel

Al	As	B	C
0.080	0.060	0.001	0.200
Ca	Co	Cr	Cu
0.001	0.011	0.061	0.028
Mn	Mo	Nb	Ni
0.900	0.018	0.014	0.044
P	Pb	S	Sb
0.017	0.032	0.012	<0.001
Si	Sn	Ta	Ti
0.044	0.011	0.023	0.005
V	Zr	Fe	
0.004	0.007	balance	

Table 3. Test Matrix for the Passivation Experiments

Material	C1018, X65
Temperature /°C	80
pH	8.0
Purge Gas	CO ₂
NaCl concentration / wt%	1
Flow conditions /rpm	300 (stirring bar)
Gas partial pressure /bar	0.53

similar—carbon steel C1018 (composition shown in Table 2). During sample cross section preparation for TEM, the sample was finished with 1 μm diamond paste. During polishing the coupons were simultaneously cooled by flushing with 2-propanol, then ultrasonicated in 2-propanol, and blow dried. The coupons were then immersed into prepared electrolytes. The test conditions are listed in Table 3. The corrosion resistance was measured using the linear polarization resistance (LPR) technique via a Gamry Inc. PC4 potentiostat.

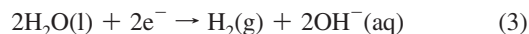
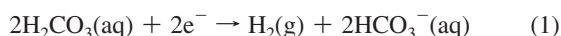
After a very brief period of bare steel surface corrosion, solid FeCO₃ was the initially formed corrosion product at the steel surface. The open circuit potential decreases as this diffusion barrier develops. The corrosion rate also decreases due to surface coverage by this scale which limits the supply of the corrosion reactants. Subsequently, spontaneous passivation was achieved as evidenced by the increased open circuit potential.⁵ The spontaneous passivation potential could be up to 400 mV higher than the initial open circuit potential for the bare metal surface. Coupons were removed from solution before and after passivation, as identified by differences in the measured corrosion potentials. They were immediately flushed with 2-propanol to dehydrate them until they cooled from 80 °C to room temperature, in order to avoid oxidation of wet films at elevated temperature. If salt precipitation (NaHCO₃ or NaCl) was observed on coupon surfaces during the cooling and drying process, they were quickly rinsed with CO₂ deaerated deionized water, then immediately flushed with 2-propanol. This removed

any deposited salts and water from the surface. Any remaining 2-propanol was blown from the surface with dry air. Samples were then stored in desiccators under a nitrogen atmosphere prior to analysis. The sample surface was analyzed by XRD and GIXRD using a Rigaku Ultima III X-ray diffractometer.

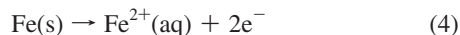
(S)TEM with EDX analysis was done on a FEITecni F20 with an EDAX EDX unit. The FEI TIA software was used to collect EDX spectral profiles. The cross-section of the surface was prepared using standard focused ion beam (FIB) techniques using ex-situ liftout (Figure 2a–d). To improve conductivity, the sample was coated with gold; a thick layer of platinum was deposited to both smooth the FeCO₃ surface and protect the cross-section during the FIB milling process. After thinning to electron transparency (Figure 2a), the cross-sectional membrane was lifted out of the trench (Figure 2b–d) and placed on a 20 nm carbon support film on a copper TEM grid.

3. Results and Discussion

3.1. Spontaneous Passivation. The electrochemical reactions on bare steel can be described as anodic (oxidation) and cathodic (reduction) half-reactions. The cathodic reactions in the present CO₂ saturated aqueous system are primarily carbonic acid reduction, proton reduction and water reduction as demonstrated by eqs 1–3:⁶



Under the conditions used here, the dominant reaction is considered to be carbonic acid reduction (1).⁶ The main anodic reaction is the oxidative dissolution of iron.



As the passivation process develops this half-reaction is likely to become slower, as evidenced by decreased corrosion rates. An open circuit potential history sample during spontaneous passivation is depicted in Figure 3 under test conditions. The open circuit potential steadily increased to a -450 mV. Classically this takes the form of an “S” shape, as has been previously reported.⁵ We speculate that the observed shape of the potential history in Figure 3 is related to phenomena associated with the nucleation and growth of the passive phase. Immediately after the sample immersion, the surface is corroding actively. Its open circuit potential is -0.777 V vs the reference electrode right before open circuit potential monitoring. The corrosion resistance is 11.8Ω . This corresponds to a corrosion rate of approximately 2.6 mm/y.⁶ This active state corresponds to point A in the schematic shown in Figure 5.

Corrosion scale, FeCO₃, gradually forms on the steel surface due to its low solubility at this pH. During this initial FeCO₃ formation, in the first 3 h, the open circuit potential decreases to -0.794 V (Figure 4), and the corrosion resistance increases to 53Ω ; this corresponds to a corrosion rate decrease to 0.5 mm/year due to the FeCO₃ scale acting as a diffusion barrier. A steel surface sample representative of this stage in the process was taken for surface analysis, and termed “sample before passivation”.

After ca. 60 h of immersion, spontaneous passivation is observed as indicated by an open circuit potential increase⁵ as depicted in Figure 3. The open circuit potential increases

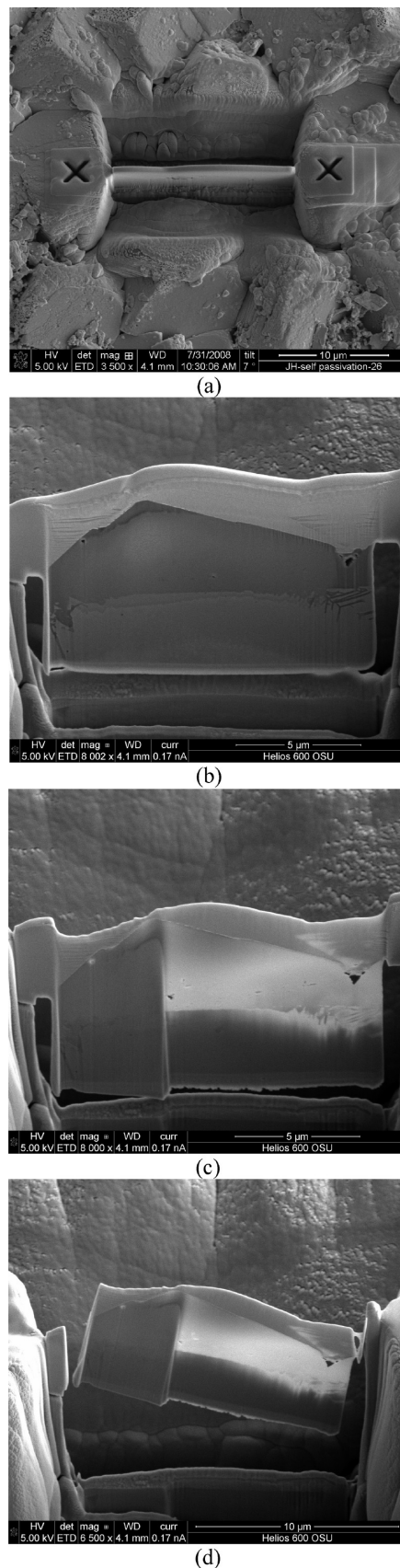


Figure 2. Crystal slice cut from the bulk surface scale by FIB.

to a value of -0.470 V vs reference electrode, and the corrosion resistance further increases to 1370Ω . This corresponds to a passivated surface as represented by point B in Figure 5.

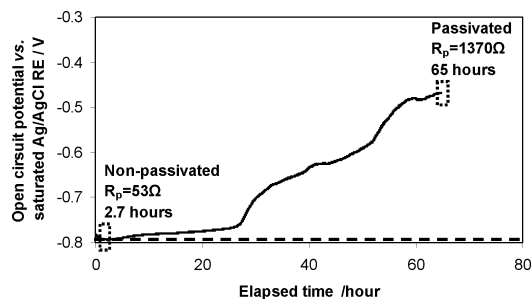


Figure 3. Open circuit potential history for spontaneous passivation.

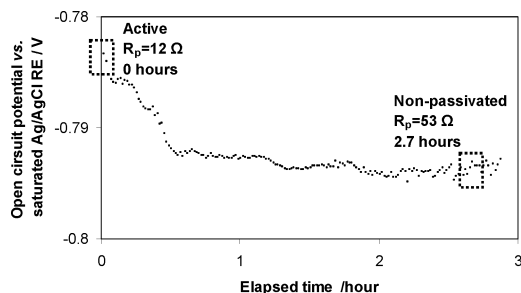


Figure 4. Open circuit potential history during initial FeCO_3 formation before passivation.

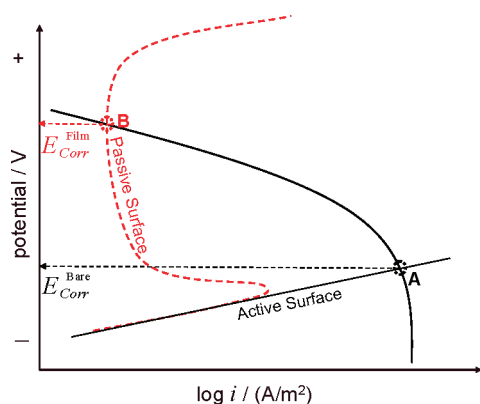


Figure 5. Sketch of a corrosion kinetics diagram showing the active-passive transition.

Coupons were prepared for XRD and GIXRD analysis before and after passivation (2.7 and 65 h immersion, respectively), as indicated by the boxes in Figure 3.

3.2. XRD and GIXRD Analysis Results. **3.2.1. Conventional X-ray Diffraction.** Conventional XRD data show the substrate iron to be dominant; iron carbonate peaks are observed from the scale before and after passivation as shown in Figures 6 and 7.¹² This is further supported by the scanning electron microscopy (SEM) images embedded in Figures 6 and 7. Acquired energy dispersive X-ray fluorescence (EDX) spectra were consistent with the formation of iron carbonate crystals. The continuously increasing incidence angle results in deeper penetration into the substrate beneath the film. Thus, a strong diffraction signal from the substrate steel is observed.

3.2.2. Grazing Incidence X-ray Diffraction. XRD with grazing incidence was employed together with the SEM to more thoroughly determine the identity of the passive film. Both SEM images before and after passivation show that the top phase is iron carbonate. The GIXRD from the sample before passivation shows that only iron carbonate peaks are present, as shown in Figure 8. The diffraction pattern only represents the outer layer;

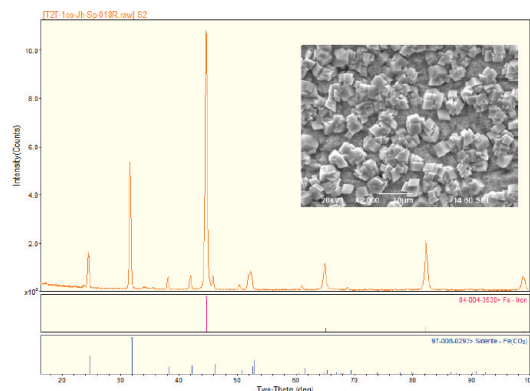


Figure 6. XRD and SEM of nonpassivated steel surface after 2.7 h of immersion.

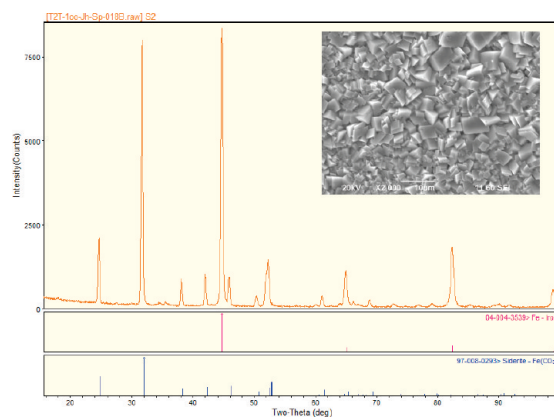


Figure 7. XRD and SEM of passivated steel surface after 65 h immersion.

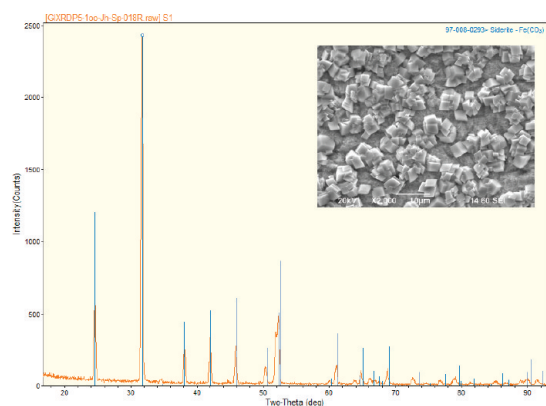


Figure 8. GIXRD and SEM of nonpassivated steel surface after 2.7 h of immersion.

therefore, diffraction from the steel substrate has been eliminated. This can be seen by comparison with Figures 6 and 7.

After the sample was passivated, an extra phase Fe_3O_4 (magnetite)¹³ along with the dominant FeCO_3 ^{12,14} was identified by GIXRD (Figure 9). The composition of the film was quantified using the Rietveld refinement technique.¹⁵ For this, the program whole pattern fitting (WPF) incorporated in diffraction data analysis software JADE8.5 was utilized. A reasonable composition with 0.4 wt % of magnetite (Fe_3O_4) and 99.6 wt % of siderite (FeCO_3) was obtained. It is therefore hypothesized here that Fe_3O_4 could be the composition of the thin passive film encountered in this environment. Since passive

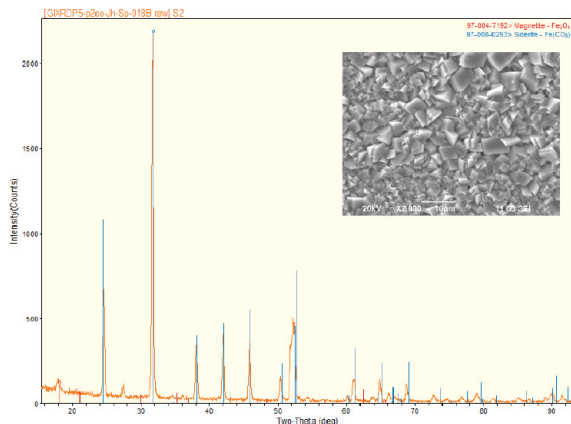


Figure 9. GIXRD and SEM of passivated metal surface after 65 h of immersion.

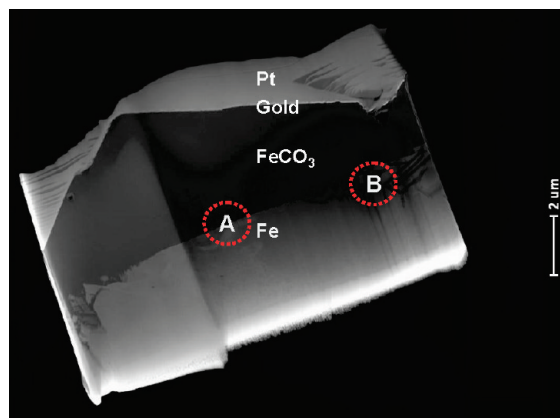


Figure 10. HAADF STEM image of a sample with circled surface A and B.

films typically have a thickness on the nanometer scale, they were difficult to observe using the conventional X-ray diffraction.

3.3. TEM/EDX Analysis Results. An image of the cross-sectional sample is shown in Figure 10. This is a high-angle annular dark-field (HAADF) STEM image where the brighter areas correspond to increased scattering of the electrons. At the top of the sample are the Pt protective layer and the gold conductive coating. Because it has a lower average atomic number, the carbonate layer is darker than the iron substrate. The interface between the iron and the iron carbonate appeared rougher at the iron grain boundaries than within the grain.

The detail from the center of the grain (location A) is shown in Figure 11. A different phase is apparent as demonstrated by a whiter color compared with steel and ferrous carbonate phase, so an STEM EDX profile was carried out using EDX at a scan step of 20 nm. The scan started from the steel substrate, went through the unknown phase, and ended at the ferrous carbonate phase as indicated by the arrow. Figure 12 shows the EDX peak intensity profile. Because elemental quantification for light elements such as carbon and oxygen is problematic, we present only the peak intensities. Compared with the Fe phase, the intensity of the oxygen signal does not change while carbon counts increase slightly in the unknown phase. This suggests that very little oxygen is in the unknown phase with carbon and iron being the primary components. Comparing the unknown and FeCO_3 phases indicates that the unknown phase has more iron, about the same carbon, and less oxygen than the FeCO_3 . We conclude that this phase is probably iron carbide

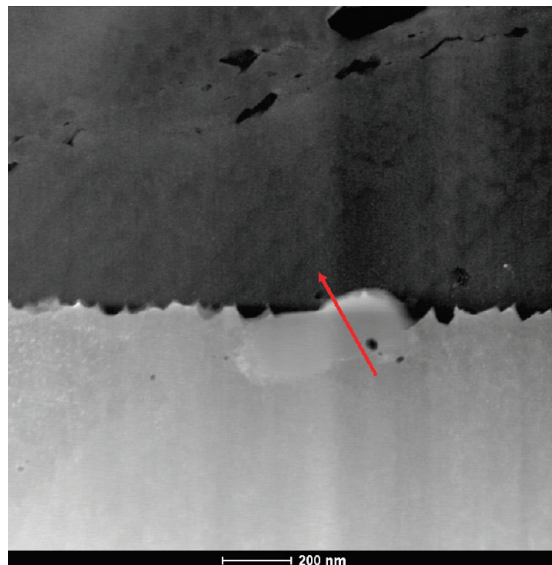


Figure 11. HAADF STEMEM image of circled area A in Figure 10 with EDX element profile indicated.

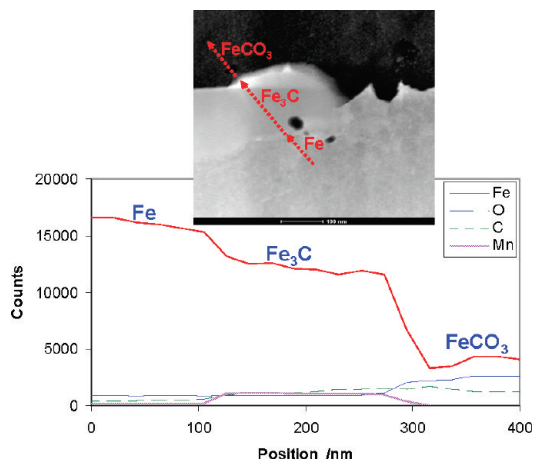


Figure 12. EDX element profile of different phases for Figure 11. Note: the unknown element was determined to be iron carbide (Fe_3C).

(Fe_3C) which was exposed as the iron from the parent steel corroded away.

At the steel grain boundary (area B in Figure 10), a much rougher interface is observed as compared with the middle part of the grain (area A). EDX analysis on area C of Figure 13 indicates the presence of manganese (see Figure 14).

An EDX profile scan was done in area D of Figure 13 (cf. the image at the top of Figure 15). As the scan steps from steel into the iron carbonate phase, higher levels of carbon and oxygen in any carbonate containing phase should be seen. The iron level in the iron carbonate should be lower than in the steel phase. The EDX results in Figure 15 clearly show these trends. A number of phases appear in area E as indicated by a gray color as compared with dark FeCO_3 and white iron phases. The thickness is estimated to be between 20–100 nm. To identify this phase, EDX scanning to profile elements was executed as indicated by the TEM image at the top of Figure 16. Compared with the pure steel phase, an obvious increase of oxygen and decrease of iron levels are observed in the unknown phase as shown in Figure 16. The carbon level is constant in both phases. This compositional relationship between carbon and oxygen rejects the hypothesis that the passive film is a carbonate containing phase. All the above information clarifies that the

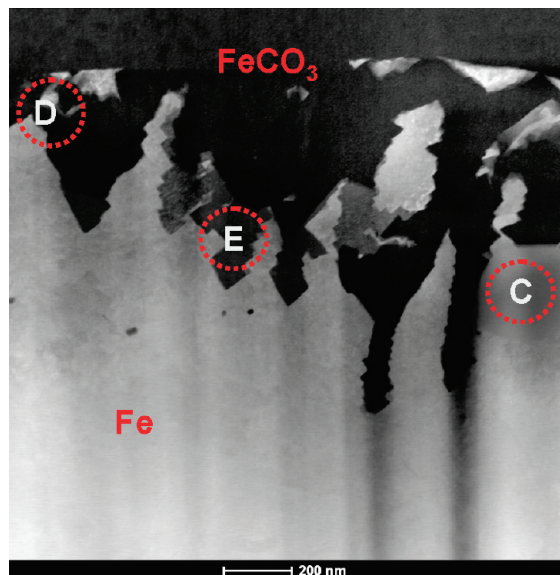


Figure 13. TEM image of edge surface of area B in Figure 10 with designated areas C, D and E for analysis.

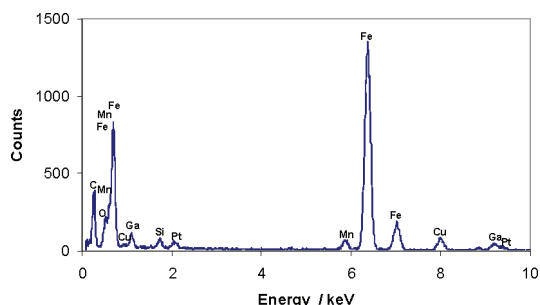


Figure 14. Alloyed element Mn is observed by EDX on area C in Figure 13.

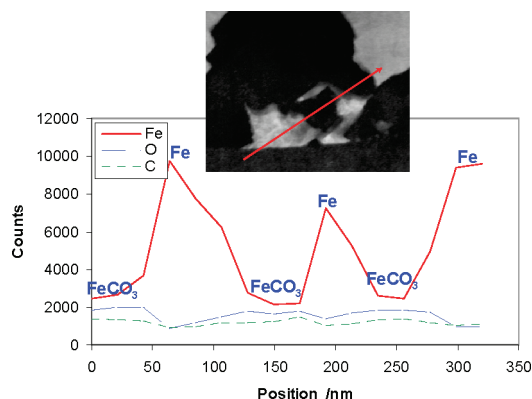


Figure 15. Element profile at different phases for area D in Figure 13. EDX directional scan indicated in TEM image.

unknown phase only contains iron and oxygen. In other words, the unknown compound is one of the iron oxides. This observation qualitatively agrees with the GIXRD results suggesting that the passive layer is magnetite (Fe_3O_4). The TEM images show that this passive film is not a continuous film covering the steel surface, but is primarily located at the boundaries between the FeCO_3 crystals. Note that the positions of the peaks and troughs for the Fe and O coincide with the different contrast regions on the TEM. This technique cannot detect hydrogen, so it cannot be used to identify the presence of any hydroxides.

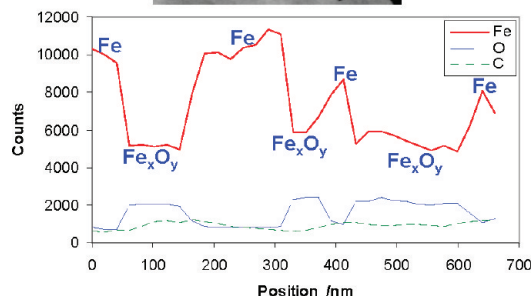
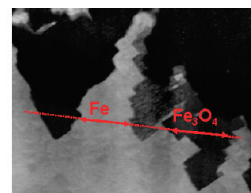


Figure 16. Element profile at different phases for Area E in Figure 13. EDX directional scan indicated in TEM image.

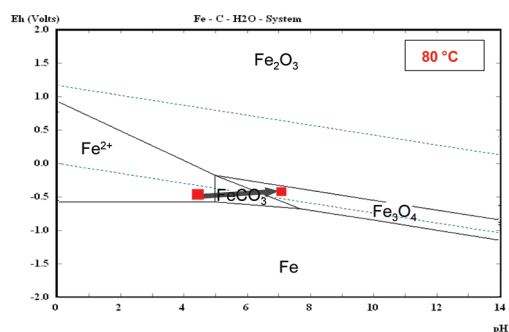


Figure 17. Simplified Pourbaix diagram showing an increase of pH and consequently potential beneath a FeCO_3 scale leading to passivation.

4. Passivation Scenario for Mild Steel in CO_2 Environments

From previous^{5,9} and current research results, it is possible now to propose a mechanism of passivation of mild steel in CO_2 aqueous electrolyte, given a high enough pH, iron carbonate can be formed when surface FeCO_3 supersaturation is achieved. As the iron carbonate scale becomes compact, it retards replenishment of protons which are consumed by corrosion at the steel surface; therefore, a higher local (surface) pH can be achieved. When it reaches a critical pH for iron oxide formation, a passivating magnetite phase is formed as follows:¹⁶



This is shown schematically in a simplified Pourbaix diagram,⁷ in Figure 17.

5. Conclusions

XRD in combination with grazing incidence diffraction (GIXRD) was applied for thin passive film identification in order to study mild steel corrosion in CO_2 aqueous environments. It was found that FeCO_3 was the dominant phase before and after passivation was observed. A trace amount of Fe_3O_4 was shown to be present after passivation. TEM/EDX showed the corrosion product FeCO_3 , an iron carbide residue, and the presence of Mn. The TEM/EDX results were

consistent with the hypothesis that the passive film is magnetite (Fe_3O_4). The TEM/EDX technique also indicated that the magnetite formed predominantly at the boundaries of FeCO_3 crystals.

Acknowledgment

The authors acknowledge the financial support from the Corrosion Center Joint Industry Project (company members, namely, Baker Petrolite, BP, Champion Technologies, Chevron, Clariant, Columbia Gas Transmission, ConocoPhillips, Eni, ExxonMobil, MI Production Chemicals, Nalco, Occidental Oil Company, Petrobras, PTTEP, Saudi Aramco, Shell, Tenaris and Total).

Literature Cited

- (1) Stepanov, S. A. Grazing-incidence X-ray diffraction. *3rd Autumn School on X-ray Scattering from Surfaces and Thin Layers*, Smolenice, Slovakia, October 1–4, 1997.
- (2) Tanner, B. K.; Hase, T. P. A.; Lafford, T. A.; Goorsky, M. S. Grazing incidence in-plane X-Ray diffraction in the laboratory. *Adv. X-ray Anal.* **2004**, *47*, 309.
- (3) Sembiring, S.; O'Connor, B.; Li, D.; van Riessen, A.; Buckley, C.; Low, I.; De Marco, R. Grazing incidence X-ray diffraction characterization of corrosion deposits induced by CO_2 on mild steel. *Adv. X-ray Anal.* **2004**, *43*, 319.
- (4) The Nobel Foundation. http://nobelprize.org/educational_games/physics/microscopes/tem/index.html (accessed Nov. 18, 2008).
- (5) Han, J.; Yang, Y.; Nescic, S.; Brown, B. Roles of passivation and galvanic effects in localized CO_2 corrosion of mild steel. *NACE CORROSION/2008*, New Orleans, LA, May 27–30, 2008; Paper No. 08332.

- (6) Nescic, S.; Postlethwaite, J.; Olsen, S. An electrochemical model for prediction of corrosion of mild steel in aqueous carbon dioxide solutions. *Corrosion* **1996**, *54* (4), 280.
- (7) Pourbaix, M. *Atlas of Electrochemical Equilibria in Aqueous (English Edition)*; Pergamon Press: Oxford, 1966.
- (8) Heuer, J. K.; Stubbins, J. F. An XPS characterization of FeCO_3 films from CO_2 corrosion. *Corros. Sci.* **1999**, *41*, p. 1231.
- (9) Han, J.; Yang, Y.; Brown, B.; Nescic, S. Electrochemical investigation of localized CO_2 corrosion on mild steel. *NACE CORROSION/2007*, Nashville, TN, March 11–15, 2007; Paper No. 07323.
- (10) De Marco, R.; Jiang, Z.; John, D.; Sercombe, M.; Kinsella, B. An in situ electrochemical impedance spectroscopy/synchrotron radiation grazing incidence X-ray diffraction study of the influence of acetate on the carbon dioxide corrosion of mild steel. *Electrochim. Acta* **2007**, *52*, 3746–3750.
- (11) Guo, X.-P.; Tomoe, Y. The effect of corrosion product layers on the anodic and cathodic reactions of carbon steel in CO_2 -saturated MDEA solutions at 100°C. *Corros. Sci.* **1999**, *41*, 391.
- (12) Han, J.; Young, D.; Nešić, S. Characterization of the Passive Film on Mild Steel in CO_2 Environments. *ICC/2008*, Las Vegas, NV, October 6–10, 2008; Paper No. 2511.
- (13) Chang, H. S. W.; Chiou, C.-C.; Chen, Y.-W. Synthesis, characterization, and magnetic properties of Fe_3O_4 thin films prepared via a sol-gel method. *J. Solid State Chem.* **1997**, *128*, 87.
- (14) Graf, D L. Crystallographic tables for the rhombohedral carbonates. *Am. Mineral.* **1961**, *46*, 1283.
- (15) Rietveld, H. M. A profile refinement method for nuclear and magnetic structures. *J. Appl. Crystallogr.* **1969**, *2*, 65.
- (16) MacDougall, B.; Graham, M. J. Growth and Stability of Passive Films. In *Corrosion Mechanisms in Theory and Practice*, 2nd ed.; Marcus, P., Ed.; Marcel Dekker, Inc.: New York, 2002; Chapter 6, p 190.

Received for review November 26, 2008
 Revised manuscript received March 19, 2009
 Accepted May 2, 2009

IE801819Y